CHEMISTRY OF MATERIALS

Article

pubs.acs.org/cm

Selectivity in Thermal Atomic Layer Etching Using Sequential, Self-Limiting Fluorination and Ligand-Exchange Reactions

Younghee Lee,[†] Craig Huffman,[‡] and Steven M. George*[,†,§]

[†]Department of Chemistry and Biochemistry, University of Colorado, Boulder, Colorado 80309, United States

[‡]SUNY Poly SEMATECH, Albany, New York 12203, United States

[§]Department of Mechanical Engineering, University of Colorado, Boulder, Colorado 80309, United States

ABSTRACT: Atomic layer etching (ALE) can result from sequential, self-limiting thermal reactions. The reactions during thermal ALE are defined by fluorination followed by ligand exchange using metal precursors. The metal precursors introduce various ligands that may transfer during ligand exchange. If the transferred ligands produce stable and volatile metal products, then the metal products may leave the surface and produce etching. In this work, selectivity in thermal ALE was examined by exploring tin(II) acetylacetonate ($Sn(acac)_2$), trimethylaluminum (TMA), dimethylaluminum chloride (DMAC), and $SiCl_4$ as the metal precursors. These metal precursors provide acac, methyl, and chloride ligands for ligand exchange. HF-pyridine was employed as the fluorination reagent. Spectroscopic ellipsometry was used to measure the etch rates of Al_2O_3, HfO_2, ZrO_2, SiO_2, Si_3N_4, and TiN thin films on silicon wafers. The spectroscopic ellipsometry measurements revealed that HfO_2 was etched by all of the metal precursors. Al_2O_3 was etched by all of the metal precursors except $SiCl_4$. ZrO_2 was etched by all of the metal precursors except TMA. In contrast, SiO_2, Si_3N_4, and TiN were not etched by any of the metal precursors. These results can be explained by the stability and volatility of the possible reaction products. Temperature can also be used to obtain selective thermal ALE. The temperature dependence of ZrO_2, HfO_2, and Al_2O_3 ALE was examined using $SiCl_4$ as the metal precursor. Higher temperatures can discriminate between the etching of ZrO_2, HfO_2, and Al_2O_3. The temperature dependence of Al_2O_3 ALE was also examined using $Sn(acac)_2$, TMA, and DMAC as the metal precursors. $Sn(acac)_2$ etched Al_2O_3 at temperatures ≥150 °C. DMAC etched Al_2O_3 at higher temperatures ≥225 °C. TMA etched Al_2O_3 at even higher temperatures ≥250 °C. The combination of different metal precursors with various ligands and different temperatures can provide multiple pathways for selective thermal ALE.

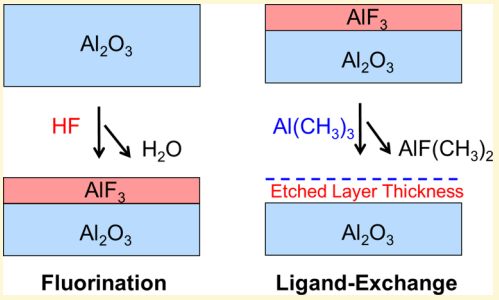

I. INTRODUCTION

Atomic layer etching (ALE) can remove thin films with atomic scale precision using sequential, self-limiting surface reactions.[1,2] Most reported ALE processes have employed halogenation reactions followed by energetic ion or noble gas atom bombardment to etch the material.[1−4] Thermal ALE processes have also been developed using sequential exposures of HF and metal precursors.[5] Thermal ALE is the reverse of atomic layer deposition (ALD).[6] Thermal ALE studies have demonstrated Al_2O_3 ALE,[7,8] HfO_2 ALE,[9] and AlF_3 ALE.[10] These thermal ALE investigations have utilized HF and $Sn(acac)_2$ as the reactants. Other recent thermal ALE studies have demonstrated Al_2O_3 ALE using HF and trimethylaluminum (TMA) as the reactants.[11]

The reactions during thermal ALE are based on gas-phase fluorination and ligand exchange as illustrated in Figure 1.[5] Fluorination first converts the metal-containing compound to the metal fluoride. Most fluorination reactions of metal-containing compounds are thermochemically favorable.[5,8] The metal precursor then undergoes a ligand-exchange reaction with the metal fluoride. The ligand exchange can be characterized as a metal exchange transmetalation reaction[12] or a redistribution reaction.[13] During the ligand-exchange reaction, the metal precursor can accept fluorine from the metal fluoride. The ligand-exchange reaction can also transfer a ligand from the metal precursor to the metal fluoride. The transition state is believed to be a four-center ring formed by the metal in the metal precursor and the metal in the metal fluoride with fluorine and ligand bridging species.[12]

If the ligand-exchange reaction produces stable and volatile metal products, then the metal products may leave the surface and produce etching. The ligand-exchange reaction may not occur or may not produce etching if the possible metal products are not stable or volatile. This difference between the stability and volatility of the possible metal reaction products can lead to selective etching. Selectivity in thermal ALE may also be achievable based on the stability of the resulting metal fluoride or by tuning the etching temperature.

Selectivity in etching is required to remove one material in the presence of other different materials.[1] Selective ALE has many applications in semiconductor device fabrication and surface cleaning.[1] The selectivity in thermal ALE may be much

Received: June 22, 2016
Revised: October 3, 2016
Published: October 4, 2016

DOI: 10.1021/acs.chemmater.6b02543
Chem. Mater. 2016, 28, 7657−7665

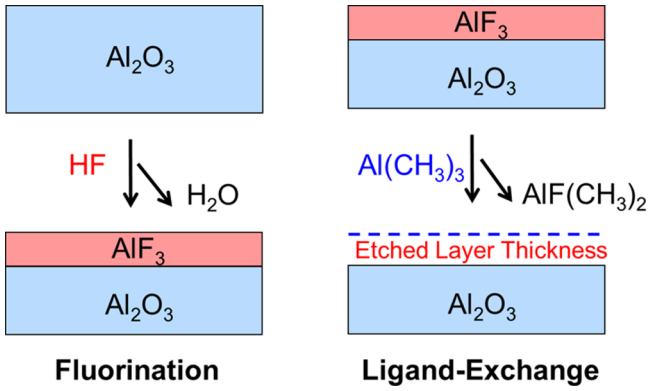

Figure 1. Schematic for Al_2O_3 ALE using HF and TMA as the reactants. HF fluorinates Al_2O_3 to form an AlF_3 layer on the surface. Subsequently, TMA accepts F from the AlF_3 layer and donates a methyl ligand to the AlF_3 layer to form volatile reaction products such as $AlF(CH_3)_2$.

higher than the selectivity during plasma ALE. The selectivity in plasma ALE depends on the energy thresholds for sputtering that are not clearly differentiated for most materials. One example of selectivity in plasma ALE is between SiO_2 and Si using fluorocarbon adsorption followed by Ar^+ ion bombardment.[4] Reasonable selectivity is observed for SiO_2 etching versus Si etching at an Ar^+ ion energy of 25 eV. However, selectivity is largely lost at the slightly higher ion energy of 30 eV.[4]

In this work, the selectivity in thermal ALE was explored using four different metal precursors for ligand exchange with HF-pyridine as the fluorination precursor. The metal precursors were tin(II) acetylacetonate ($Sn(acac)_2$), trimethylaluminum (TMA), dimethylaluminum chloride (DMAC), and silicon tetrachloride ($SiCl_4$). These metal precursors can transfer acac, methyl, and chloride ligands during the ligand-exchange reaction. These reactants were used to etch Al_2O_3, HfO_2, ZrO_2, SiO_2, Si_3N_4, and TiN thin films on silicon wafers. These six materials are all important in semiconductor device processing. Spectroscopic ellipsometry was then employed to measure the film thicknesses versus number of ALE cycles for each of the six materials. These experiments were able to determine the selectivity of thermal ALE to the different materials using the various metal precursors and the relative etch rates.

Additional experiments explored the selectivity of thermal ALE resulting from substrate temperature. The etching of HfO_2, ZrO_2, and Al_2O_3 at different temperatures was explored using $SiCl_4$ as the molecular precursor. Al_2O_3 ALE was also examined at various temperatures using $Sn(acac)_2$, DMAC, and TMA as the metal precursors. These etching studies revealed that temperature can provide an additional pathway for selective thermal ALE.

II. EXPERIMENTAL SECTION

The thermal ALE reactions were performed in a viscous flow ALD reactor.[14] The reaction temperatures from 150 to 350 °C were maintained by a proportional-integral-derivative (PID) temperature controller (2604, Eurotherm). The pressure was monitored by a capacitance manometer (Baratron 121A, MKS). A constant flow of 150 sccm of ultra high purity (UHP) N_2 gas was supplied by mass flow controllers (Type 1179A, MKS). This N_2 gas flow produced a base pressure of ∼1 Torr in the reactor pumped by a mechanical pump (Pascal 2015SD, Alcatel).

The fluorination reaction employed a HF-pyridine solution (70 wt % HF, Sigma-Aldrich) as the HF source. The HF-pyridine solution has an equilibrium with gaseous HF. The vapor pressure of HF over the HF-pyridine solution is 90−100 Torr at room temperature.[9] Only gaseous HF, without measurable pyridine vapor, is observed in the gas phase.[15] HF derived from the HF-pyridine solution avoids the difficulty of handling high pressure HF gas cylinders. The HF-pyridine solution was transferred to a gold-plated stainless steel bubbler in a dry N_2-filled glovebag. The HF-pyridine solution was held at room temperature. The pressure transients of HF derived from the HF-pyridine source were adjusted to ∼80 mTorr using a metering bellows-sealed valve (SS-4BMG, Swagelok).

The metal precursors for the ligand-exchange reaction were tin(II) acetylacetonate ($Sn(acac)_2$, 37−38% Sn, Gelest), trimethylaluminum (TMA) (97%, Sigma-Aldrich), dimethylaluminum chloride (DMAC) (97%, Sigma-Aldrich), and silicon tetrachloride ($SiCl_4$) (98%, Gelest). The $Sn(acac)_2$ precursor was maintained at 100 °C. The $Sn(acac)_2$ pressure transients were adjusted to ∼20 mTorr using a metering valve. The TMA, DMAC, and $SiCl_4$ precursors were held at room temperature. The TMA and DMAC pressure transients were regulated at ∼40 mTorr using metering valves. The $SiCl_4$ pressure transients were defined at ∼120 mTorr also using a metering valve. The etch rates reached constant values at longer metal precursor exposures using these pressure transients.

Various thin films on silicon wafers were prepared by SEMATECH to measure the etch rates during thermal ALE. The TiN, Al_2O_3, HfO_2, and ZrO_2 films were deposited by semiconductor ALD processes in commercially available tools. Chemical vapor deposition was employed to prepare the SiO_2 and Si_3N_4 films using typical process conditions in a high volume single wafer tool. The thickness of all the initial films was targeted to be ∼50 Å. Actual thicknesses were in the range of 39−68 Å as determined by spectroscopic ellipsometry (SE) measurements. The ALE experiments were performed in parallel by placing the Al_2O_3, HfO_2, ZrO_2, SiO_2, Si_3N_4, and TiN thin films on silicon wafers in the viscous flow reactor. For each experiment, there was one sample for each of the six materials. The six samples were each 1.25 cm by 1.25 cm in size.

The ALE reactions were performed using an optimized reaction sequence. This reaction sequence is represented as x−30−1−30 and consists of an exposure of metal precursor for x s, 30 s of N_2 purge, 1 s of HF exposure derived from the HF-pyridine solution, and 30 s of N_2 purge. The ALE reactions using $Sn(acac)_2$ as a metal precursor were performed using a reaction sequence of 1−30−1−30. The ALE reactions using TMA, DMAC, or $SiCl_4$ as the metal precursor were performed using a reaction sequence of 2−30−1−30. The reaction sequence is optimized when an additional increase in the exposure of the metal precursor does not produce a higher etch rate.

The thicknesses of the various films were measured by SE measurements. A spectroscopic ellipsometer (M-2000, J. A. Woollam) measured Ψ and Δ at 240−900 nm with an incidence angle of 75°. The analysis software (CompleteEASE, J. A. Woollam) fitted Ψ and Δ to determine the thicknesses and refractive index of the film. A Sellmeier model was used for fitting the thickness of the Al_2O_3, HfO_2, ZrO_2, SiO_2, and Si_3N_4 films. A Lorentz model was used for fitting the TiN film. The film thickness versus number of ALE cycles determined the etch rate. Based on least-squares fitting of the film thicknesses versus number of ALE cycles, the reported etch rates are accurate to within ±0.01 Å/cycle. Most of the individual least-squares fittings are accurate to within ±0.005 Å/cycle.

The temperature-dependent ALE experiments on Al_2O_3 were performed using an in situ quartz crystal microbalance (QCM) in the viscous flow ALD reactor.[14] The quartz crystal (gold coated and polished, RC crystal, 6 MHz, Phillip Technologies) was placed in a sensor head (BSH-150, Inficon) and then sealed with high temperature epoxy (Epo-Tek H21D, Epoxy technology). The mass changes during the ALE reactions were recorded by a thin film deposition monitor (Maxtek TM-400, Inficon).[7,8] The initial Al_2O_3 films were grown on the QCM crystal using Al_2O_3 ALD with TMA and H_2O as the reactants at the same temperature as the ALE reactions.

DOI: 10.1021/acs.chemmater.6b02543
Chem. Mater. 2016, 28, 7657−7665

III. RESULTS AND DISCUSSION

A. Results for Selectivity Based on Metal Precursor. The etching results using $Sn(acac)_2$ as the metal precursor are presented in Figure 2. Figure 2a shows the SE measurements of the film thicknesses after 50, 100, 200, and 400 ALE cycles using sequential HF and $Sn(acac)_2$ exposures at 200 °C. The Al_2O_3, ZrO_2, and HfO_2 films were etched linearly versus the number of ALE cycles. In contrast, there were no measurable thickness changes for the SiO_2, Si_3N_4, and TiN films. Figure 2b displays the film thickness versus the number of ALE cycles for the Al_2O_3, ZrO_2, and HfO_2 films. The slopes from the linear least-squares fittings of the data in Figure 2b yielded etch rates of 0.23 Å/cycle, 0.14 Å/cycle, and 0.06 Å/cycle for the Al_2O_3, ZrO_2, and HfO_2 films, respectively. The etch rates of Al_2O_3 and HfO_2 are consistent with earlier reported values.[7−9] The etch rate of ZrO_2 was determined for the first time.

Additional control experiments were performed on the Al_2O_3, ZrO_2, and HfO_2 films to determine if both HF and $Sn(acac)_2$ were necessary for the thermal ALE. Experiments using 200 cycles of HF exposures observed negligible thickness changes for the Al_2O_3, ZrO_2, and HfO_2 films. In addition, sequential exposures of HF and acetylacetone (acacH, Sigma-Aldrich >99%) did not lead to the etching of Al_2O_3 at 200 °C. Without the metal acetylacetonate precursor, acetylacetone alone does not yield thermal ALE.

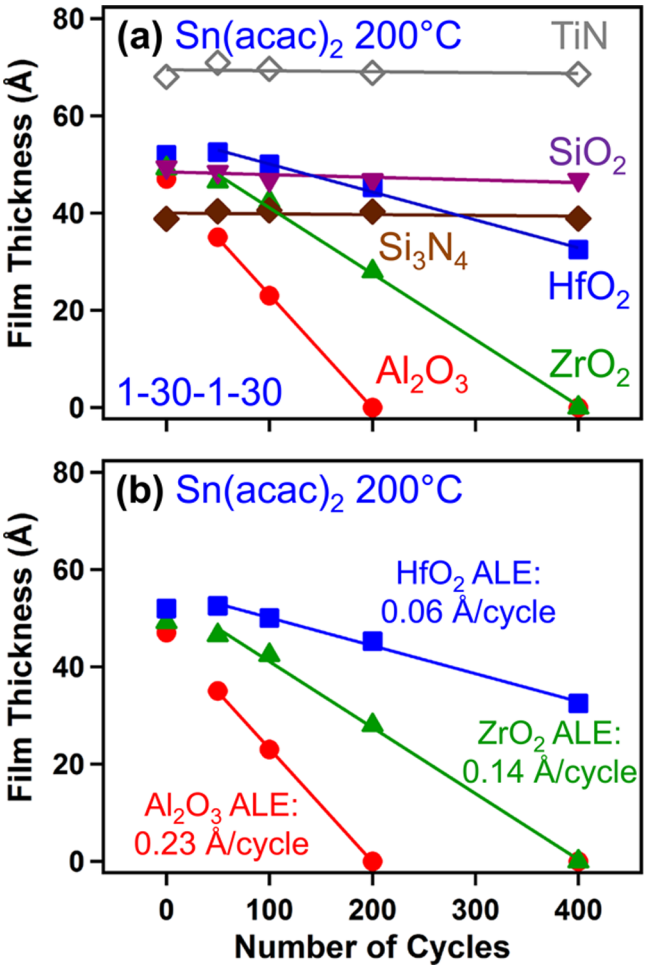

Figure 2. (a) Film thickness versus number of HF and $Sn(acac)_2$ reaction cycles at 200 °C for a variety of materials. (b) Film thickness versus number of HF and $Sn(acac)_2$ reaction cycles at 200 °C for Al_2O_3, HfO_2, and ZrO_2 showing etch rates.

Both the metal and the ligands on the metal precursor were changed for the results for TMA shown in Figure 3. Figure 3a displays the film thicknesses after 25, 50, 100, and 200 ALE cycles using sequential HF and TMA exposures at 300 °C. The Al_2O_3 and HfO_2 films were etched linearly versus the number of ALE cycles. There were negligible thickness changes during 200 ALE cycles for the ZrO_2, SiO_2, Si_3N_4, and TiN films. The film thicknesses versus the number of ALE cycles for the Al_2O_3, HfO_2, and ZrO_2 films are shown in Figure 3b. Etch rates of 0.45 Å/cycle and 0.10 Å/cycle were measured for the Al_2O_3 and HfO_2 films, respectively. The etch rate of Al_2O_3 is in agreement with the value measured earlier by quartz crystal microbalance (QCM) and SE experiments.[11] The etch rate of HfO_2 using HF and TMA was determined for the first time. A negligible etch rate of 0.01 Å/cycle was determined for the ZrO_2 film.

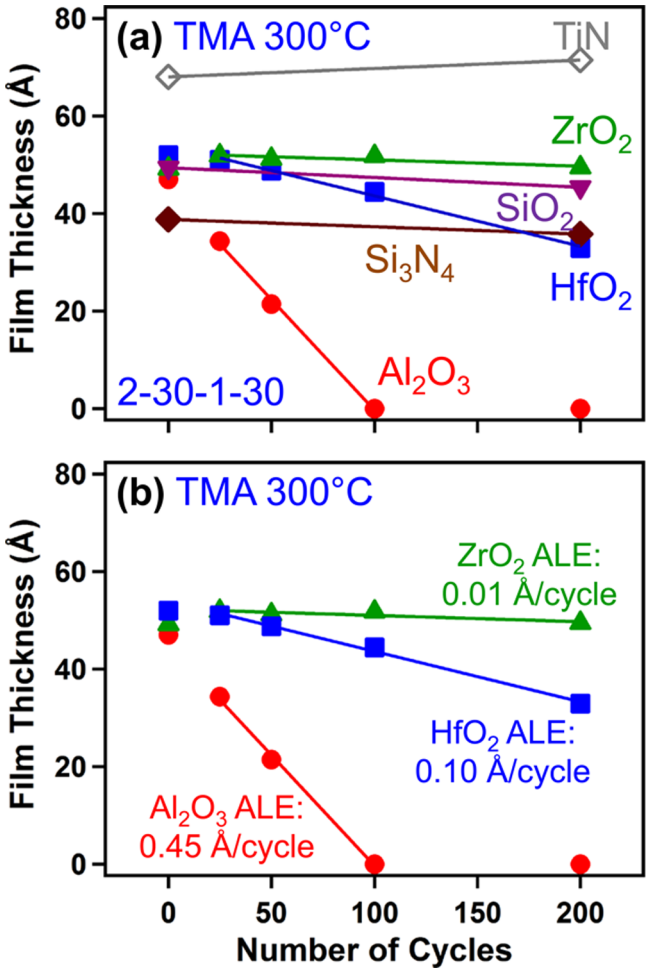

Figure 3. (a) Film thickness versus number of HF and TMA reaction cycles at 300 °C for a variety of materials. (b) Film thickness versus number of HF and TMA reaction cycles at 300 °C for Al_2O_3, HfO_2, and ZrO_2 showing etch rates.

The metal remained Al and the ligands on the metal precursor were either chlorine or methyl for the results for DMAC that are displayed in Figure 4. Figure 4a shows the film thicknesses after 10, 25, 50, and 100 ALE cycles using sequential HF and DMAC exposures at 250 °C. Linear etching was observed for the ZrO_2, HfO_2, and Al_2O_3 films versus the

DOI: 10.1021/acs.chemmater.6b02543
Chem. Mater. 2016, 28, 7657−7665

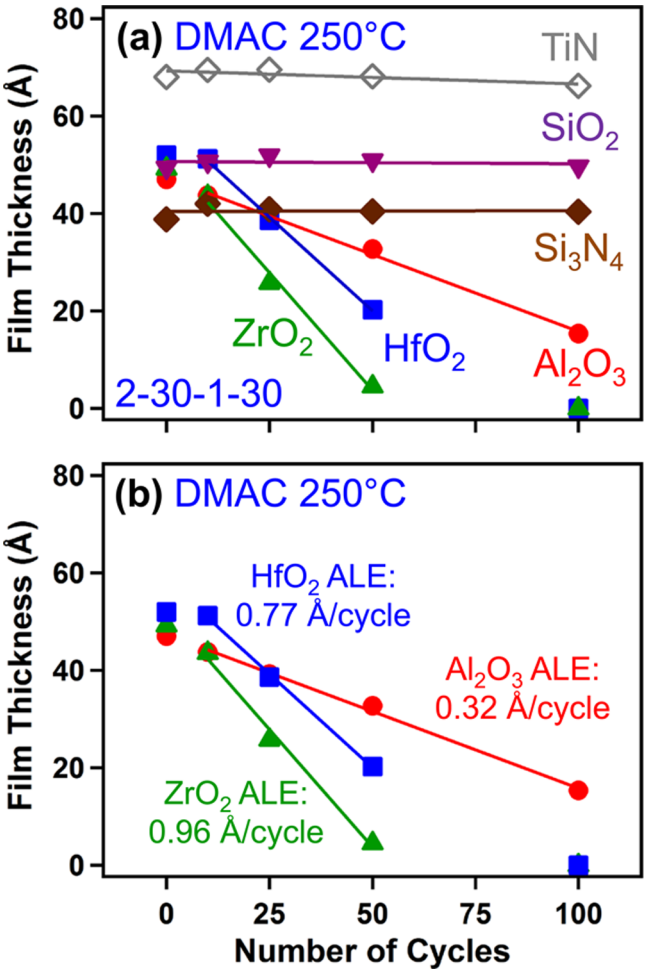

Figure 4. (a) Film thickness versus number of HF and DMAC reaction cycles at 250 °C for a variety of materials. (b) Film thickness versus number of HF and DMAC reaction cycles at 250 °C for Al_2O_3, HfO_2, and ZrO_2 showing etch rates.

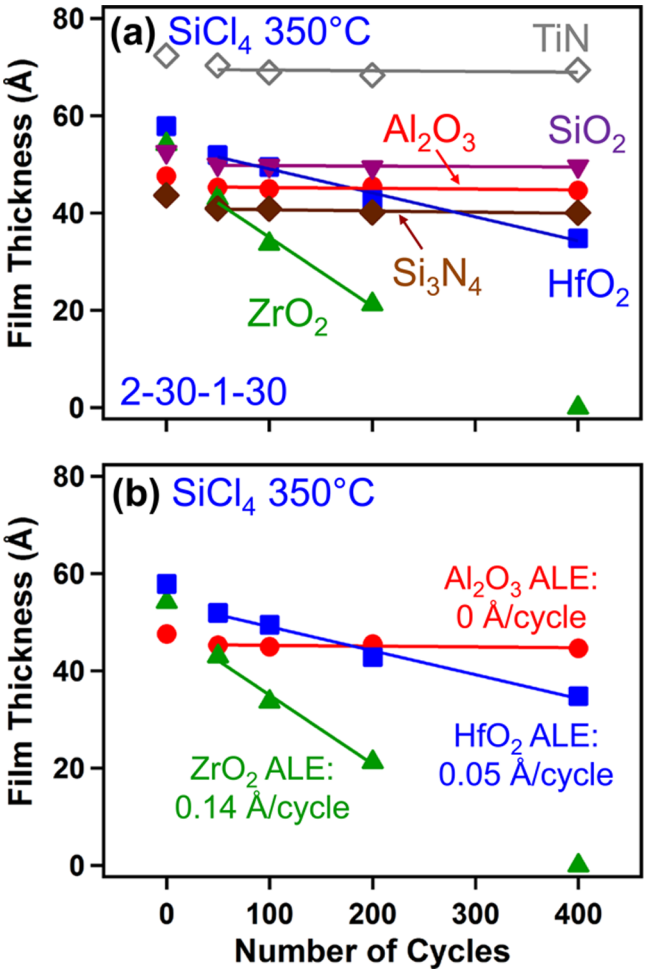

Figure 5. (a) Film thickness versus number of HF and $SiCl_4$ reaction cycles at 350 °C for a variety of materials. (b) Film thickness versus number of HF and $SiCl_4$ reaction cycles at 350 °C for Al_2O_3, HfO_2, and ZrO_2 showing etch rates.

number of ALE cycles. No measurable thickness changes were observed for the SiO_2, Si_3N_4, and TiN films. The film thicknesses versus the number of ALE cycles are displayed for the ZrO_2, HfO_2, and Al_2O_3 films in Figure 4b. Etch rates of 0.96 Å/cycle, 0.77 Å/cycle, and 0.32 Å/cycle were determined for the ZrO_2, HfO_2, and Al_2O_3 films, respectively.

The metal was changed to Si and the ligands on the metal precursor were chlorine for the results for $SiCl_4$ that are shown in Figure 5. Figure 5a displays the film thicknesses after 50, 100, 200, and 400 ALE cycles using sequential HF and $SiCl_4$ exposures at 350 °C. The ZrO_2 and HfO_2 films were etched linearly versus the number of ALE cycles. In contrast, there were no measurable thickness changes during 400 ALE cycles for the Al_2O_3, SiO_2, Si_3N_4, and TiN films. Figure 5b displays the film thickness versus the number of ALE cycles for the ZrO_2, HfO_2, and Al_2O_3 films. Etch rates of 0.14 Å/cycle and 0.05 Å/cycle were measured for the ZrO_2 and HfO_2 films, respectively. The etch rate of Al_2O_3 was negligible.

The etching results for $SiCl_4$ shown in Figure 5 were performed under self-limiting conditions. To confirm self-limiting behavior, etch rates were measured versus increasing exposure times of $SiCl_4$ while keeping the HF exposure time constant at 1.0 s. These results are shown in Figure 6a. The etch rates for both ZrO_2 and HfO_2 are self-limiting versus $SiCl_4$ exposure. The etch rates are constant at progressively larger $SiCl_4$ exposure times. The etch rates at each $SiCl_4$ exposure time were determined using at least 3–4 measured film thicknesses after different numbers of ALE cycles.

The etch rates were also determined versus increasing exposure times of HF while maintaining a constant $SiCl_4$ exposure time of 2.0 s. These results are displayed in Figure 6b. The etch rate for HfO_2 is self-limiting versus HF exposures. In addition, the etch rate for ZrO_2 begins to level off at higher HF exposures. The slight increases at larger HF exposures for ZrO_2 can be attributed to the difficulty purging HF from the reactor after longer HF exposures. Residual HF remaining in the reactor will lead to chemical vapor etching (CVE) during the $SiCl_4$ exposure. Similar influences of CVE on thermal ALE have been observed earlier after longer HF exposures.[8,9]

Al_2O_3 ALE is self-limiting using HF and $Sn(acac)_2$ exposures[8] or HF and TMA exposures.[11] HfO_2 ALE is also known to be self-limiting using HF and Sn(acac) exposures.[9] Additional studies have confirmed that Al_2O_3 ALE is self-limiting using HF and DMAC exposures. ZrO_2 ALE using HF and $Sn(acac)_2$ exposures, HfO_2 or ZrO_2 ALE using HF and DMAC exposures and HfO_2 ALE using HF and TMA exposures were run under the same self-limiting reaction conditions as employed for Al_2O_3 ALE.

DOI: 10.1021/acs.chemmater.6b02543
Chem. Mater. 2016, 28, 7657−7665

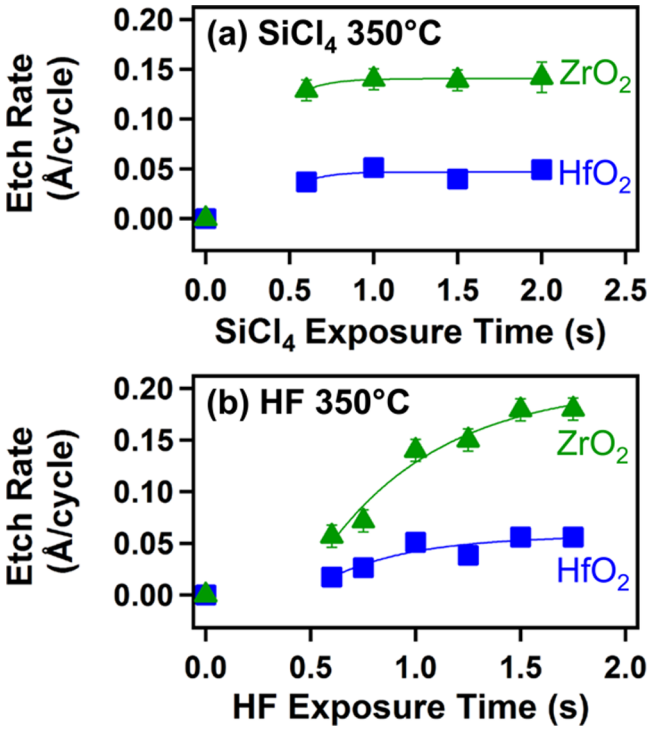

Figure 6. (a) Etch rates for ZrO_2 and HfO_2 versus $SiCl_4$ exposure time with constant HF exposure time of 1.0 s. (b) Etch rates for ZrO_2 and HfO_2 versus HF exposure time with constant $SiCl_4$ exposure time of 2.0 s.

The etch rates from the results in Figures 2−5 are less than the unit cell length or a "monolayer" of the various materials. The thermal ALE process removes material progressively based on the fluorination and ligand-exchange reactions. The amount etched in one ALE cycle is determined by how much material is fluorinated and then how much of the metal fluoride is removed by ligand exchange. A similar situation occurs for ALD where the growth per ALD cycle is usually less than the unit cell length or a "monolayer" of the material.[16] In the case of ALD, the growth limits are defined primarily by the number surface sites that can react with the ALD precursors.[6]

B. Discussion of Selectivity Based On Metal Precursor. Figures 2-5 illustrate that the etching depends on both the material and the metal precursor. The etching results can be explained by the stability and volatility of the reaction products. The Al_2O_3, ZrO_2, and HfO_2 films were etched by most of the metal precursors. The fluorination of Al_2O_3, HfO_2, and ZrO_2 by HF is thermochemically favorable. The reaction Al_2O_3 + $6HF(g) \rightarrow 2AlF_3 + 3H_2O(g)$ has ΔG values of −58.4, −53.8, −49.1, and −44.4 kcal/mol at 200, 250, 300, and 350 °C, respectively.[17] The reaction $HfO_2 + 4HF(g) \rightarrow HfF_4 + 2H_2O(g)$ has ΔG values of −19.1, −16.0, −12.8, and −9.6 kcal/mol at 200, 250, 300, and 350 °C, respectively.[17] The reaction $ZrO_2 + 4HF(g) \rightarrow ZrF_4 + 2H_2O(g)$ has ΔG values of −18.4, −15.2, −12.1, and −8.9 kcal/mol at 200, 250, 300, and 350 °C, respectively.[17] The resulting AlF_3, HfF_4, and ZrF_4 reaction products are not volatile. AlF_3, HfF_4, and ZrF_4 sublime at 1276, 970, and 912 °C, respectively.[18]

The subsequent ligand-exchange reactions can produce stable and volatile reaction products for most of the metal precursors with the AlF_3, HfF_4, and ZrF_4 metal fluorides. For example, for the $Sn(acac)_2$ results shown in Figure 2, $Sn(acac)_2$ can accept F and donate acac to produce volatile SnF(acac) and metal products with acac ligands. This ligand exchange is facilitated by the ability of fluorine to form bimetallic bridges.[19] The acac ligand from $Sn(acac)_2$ can form stable metal acetylacetonate compounds with Al, Hf, and Zr. $Al(acac)_3$ has a vapor pressure of ∼3 Torr at 150 °C.[20] $Hf(acac)_4$ and $Zr(acac)_4$ have vapor pressures > ∼0.1 Torr at 150 °C.[21] The exact metal products have not yet been identified with mass spectrometry. Metal fluoro(acetylacetonate) etch products are also possible. Related chloro(acetylacetonate) compounds have been characterized such as SnCl(acac) and $AlCl_2(acac)$.[22,23] Additional halo(acetylacetonate) compounds have also been reported such as $HfX(acac)_3$, $HfX_2(acac)_2$, $ZrX(acac)_3$, and $ZrX_2(acac)_2$ where X = Cl or Br.[24,25]

For the TMA results displayed in Figure 3, TMA can etch Al_2O_3 and HfO_2. In contrast, TMA can not etch ZrO_2. The methyl ligand from TMA can form stable metal methyl compounds with Al and Hf. TMA can accept F from AlF_3 and donate CH_3 producing volatile $AlF(CH_3)_2$ from TMA and metal products with methyl ligands from AlF_3. The possible four-center transition state for the ligand-exchange reaction between TMA and AlF_3 is shown in Figure 7a. The vapor pressure of $AlF(CH_3)_2$ is 80 Torr at 100 °C.[26] $AlF(CH_3)_2$ has been characterized as a tetramer in the gas phase.[27] $AlF(CH_3)_2$ may also be the favored metal reaction product derived from AlF_3. TMA can also accept F from HfF_4 and donate CH_3 to HfF_4 to produce volatile $AlF(CH_3)_2$ and Hf reaction products with methyl ligands. Tetramethylhafnium $Hf(CH_3)_4$ has been prepared but is known to be unstable at > −30 °C.[28] The presence of F together with the CH_3 ligand may stabilize the $HfF_x(CH_3)_{4-x}$ etch products.

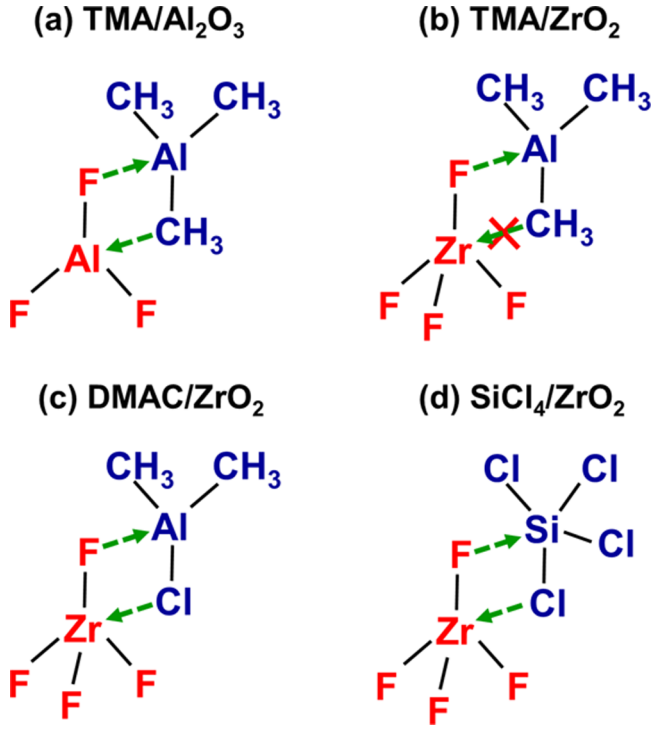

Figure 7. Possible four-center transition states for (a) TMA with AlF_3; (b) TMA with ZrF_4; (c) DMAC with ZrF_4; and (d) $SiCl_4$ with ZrF_4.

In contrast, Figure 3 illustrates that TMA does not etch the ZrO_2 film. This result is somewhat surprising because Zr and Hf generally share many chemical properties due to their similar atomic and ionic radii. However, the stability of

DOI: 10.1021/acs.chemmater.6b02543
Chem. Mater. 2016, 28, 7657−7665

$Hf(CH_3)_4$ is known to be larger than $Zr(CH_3)_4$.[29] The Hf−CH_3 bond energy is also larger than the Zr−CH_3 bond energy.[30] $Zr(CH_3)_4$ has been prepared but decomposes even at low temperatures ≤15 °C.[31] The lack of etching of ZrO_2 by sequential HF and TMA exposures may result from no methyl ligand transfer from TMA to ZrF_4 in the possible four-center transition state displayed in Figure 7b.

Although TMA did not etch ZrO_2, DMAC was able to etch ZrO_2 effectively as shown in Figure 4. The difference between TMA and DMAC is the chloride ligand on DMAC. The chloride ligand may form Al−Cl−Zr bridge species that facilitate etching.[32] These Al−Cl−Zr bridge species are illustrated in the proposed four-center transition state for ligand exchange between DMAC and ZrF_4 in Figure 7c. The chloride ligand may also promote the stability or volatility of the Zr reaction products. DMAC is known to be a good fluoride acceptor and chloride donor when reacting with Hf and Zr fluorides.[33] Hf and Zr form stable volatile metal chlorides. $HfCl_4$ and $ZrCl_4$ sublime at 317 and 331 °C, respectively.[18] The presence of Cl in the metal precursor may also stabilize the etch products. $ZrCl_2(CH_3)_2$ and $ZrCl_3(CH_3)$ are much more stable than $Zr(CH_3)_4$.[34]

Figure 5 shows that $SiCl_4$ is also able to etch ZrO_2. Together with the results for DMAC, these results argue that the chloride ligand is responsible for forming stable and volatile Zr reaction products. The possible four-center transition state for ligand exchange between $SiCl_4$ and ZrF_4 is displayed in Figure 7d. This ligand exchange would again form stable and volatile Zr chlorides.

The most surprising result in Figure 5 is the lack of Al_2O_3 etching by $SiCl_4$. ZrO_2 and HfO_2 were both etched by sequential $SiCl_4$ and HF exposures. Zr and Hf are both known to form volatile metal chlorides. Al can also form volatile metal chlorides such as $AlCl_3$. The lack of Al_2O_3 etching by $SiCl_4$ led to the exploration of alternative explanations involving the reaction thermochemistry. The thermochemistry of the ligand exchange was determined assuming complete ligand exchange to form SiF_4 and the fully chlorinated metal in the original metal fluoride.

The thermochemical results for the ligand exchange between $SiCl_4$ and AlF_3, ZrF_4 and HfF_4 are given in Figure 8. These results reveal that the ligand exchange between $SiCl_4$ and ZrF_4 or HfF_4 is thermochemically favorable at >200 °C. In contrast, the ligand exchange between $SiCl_4$ and AlF_3 is not thermchemically favorable at any temperature shown in Figure 8. These results are consistent with the results in Figure 5. ZrF_4 and HfF_4 can both undergo ligand exchange with $SiCl_4$ at 350 °C because these reactions are spontaneous with $\Delta G \approx -10$ kcal/mol. On the other hand, Al_2O_3 can not be etched at 350 °C because the ligand exchange between $SiCl_4$ and AlF_3 is not spontaneous with $\Delta G \approx +26$ kcal/mol.

In contrast to the results for Al_2O_3, HfO_2 and ZrO_2, SiO_2 and Si_3N_4 were not etched by any of the metal precursors under the reported reaction conditions. The formation of SiF_4 from SiO_2 and Si_3N_4 by reaction with HF is thermochemically favorable. The reaction $SiO_2 + 4HF(g) \rightarrow SiF_4(g) + 2H_2O(g)$ has ΔG values of −14.0, −13.0, and −12.0 kcal/mol at 200, 250, and 300 °C, respectively.[17] The reaction $Si_3N_4 + 12HF(g) \rightarrow 3SiF_4(g) + 4NH_3(g)$ has ΔG values of −159.9, −153.2, and −146.5 kcal/mol at 200, 250, and 300 °C, respectively.[17] Both of these reactions produce SiF_4 as a reaction product. SiF_4 is extremely volatile. However, neither SiO_2 nor Si_3N_4 is etched spontaneously by HF. The fluorination of SiO_2 or Si_3N_4 does not proceed all the way to SiF_4. In agreement with these results, HF does not etch SiO_2 in the absence of H_2O.[35,36]

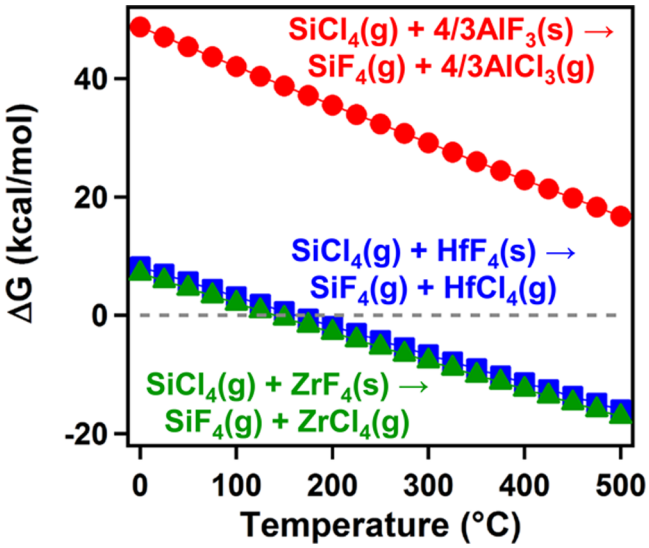

Figure 8. Thermochemical calculations for the ligand-exchange reactions between $SiCl_4$ and AlF_3, HfF_4 and ZrF_4. Ligand exchange is assumed to proceed completely to SiF_4 and the corresponding metal chloride.

Another explanation for the lack of etching of SiO_2 and Si_3N_4 is that the ligand-exchange reactions for Si−F species are not favorable. The Si−F bond is a very strong. The Si−F bond in F_3Si-F has a bond strength of 167 kcal/mol.[37] The activation energy for breaking the Si−F bond may be too high for an effective ligand-exchange reaction. Large Si−F bond strengths also lead to large activation energies for the hydrolysis of SiF_4.[38]

Ligand exchange may also not occur for the Si-compounds because the resulting reaction products are unstable. Si(IV) favors coordination numbers of four or six. The production of $Si(acac)_4$ when using $Sn(acac)_2$ as the metal precursor is not possible because this complex requires eight coordination. The requirements for Si acetylacetonates lead to a monodentating acac ligand or a cationic product such as $Si(acac)_3^+$.[39] In contrast, Si could form stable $Si(CH_3)_4$ when using TMA as the metal precursor. Si could also form $Si(CH_3)_4$ or $SiCl_4$ when using DMAC as the metal precursor. Consequently, the lack of etching of SiO_2 and Si_3N_4 is probably explained by the high activation barrier to break Si−F bonds during ligand exchange.

TiN was also not etched by any of the metal precursors. The formation of TiF_3 from TiN by HF is thermochemically favorable. The reaction $TiN + 3HF(g) \rightarrow TiF_3 + NH_3(g)$ has ΔG values of −40.3, −37.0, and −33.8 kcal/mol at 200, 250, and 300 °C.[17] The ligand-exchange reaction between TiF_3 and $Sn(acac)_2$ may also be possible. The production of $Ti(acac)_3$ from TiN when using $Sn(acac)_2$ should be feasible based on earlier studies that have prepared $Ti(acac)_3$.[40] In contrast, the production of $Ti(CH_3)_3$ from TiF_3 when using TMA as the metal precursor is not expected because there are no previous reports for $Ti(CH_3)_3$ in the literature. Likewise, the production of $TiCl_3$ from TiF_3 when using DMAC or $SiCl_4$ as the metal precursor may not be viable because $TiCl_3$ has low volatility with a boiling point of 960 °C.[18]

In addition to the absence of stable or volatile Ti(III) reaction products, the lack of etching of TiN may be explained by a TiN_xO_y or TiO_2 layer on the TiN surface.[41,42] In this case, HF would be required to fluorinate a Ti(IV) surface species.

DOI: 10.1021/acs.chemmater.6b02543
Chem. Mater. 2016, 28, 7657−7665

This reaction is nearly thermochemically neutral.[17] The formation of $Ti(acac)_4$ when using $Sn(acac)_2$ as the metal precursor for ligand exchange is also not favorable. Producing $Ti(acac)_4$ is not possible because this reaction product requires eight coordination. Ti(IV) acetylacetonate compounds favor six coordination with complexes such as Ti(=O) $(acac)_2$ and $TiCl_2(acac)_2$.

The production of $Ti(CH_3)_4$ from TiF_4 when using TMA as the metal precursor is also not expected because $Ti(CH_3)_4$ decomposes at low temperatures ≤78 °C.[34] In contrast, the production of $TiCl_4$ or $TiCl_yF_{4-y}$ from TiF_4 when using DMAC or $SiCl_4$ as the metal precursor is possible because $TiCl_4$ is a stable and volatile molecule. On the basis of these chemical arguments, the negligible etching of TiN by $Sn(acac)_2$, TMA, DMAC, or $SiCl_4$ is attributed to either the absence of stable or volatile Ti(III) reaction products or the difficulty of fluorinating Ti(IV) surface species using HF.

C. Selectivity Based On Temperature. Temperature is also an important variable for selective thermal ALE. The temperature-dependent etch rates of ZrO_2, HfO_2, and Al_2O_3 using sequential HF and $SiCl_4$ exposures are shown in Figure 9.

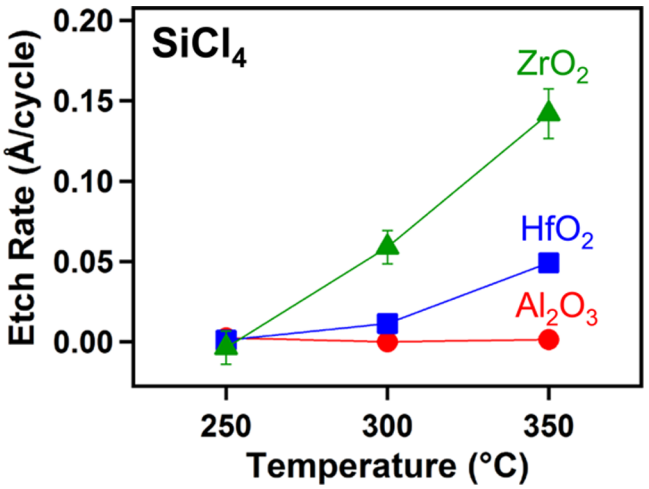

Figure 9. Etch rates of ZrO_2, HfO_2, and Al_2O_3 versus temperature using $SiCl_4$ as the metal precursor.

None of the three metal oxides is etched at 250 °C. The etch rates for ZrO_2 and HfO_2 become measurable at 300 °C. The etch rates at 350 °C were obtained from Figure 5. The etch rate of ZrO_2 is larger than HfO_2 at both 300 and 350 °C. The etch rate of Al_2O_3 is not measurable at any of the three temperatures.

The results in Figure 9 are consistent with the thermochemical calculations in Figure 8. The ligand-exchange reaction between $SiCl_4$ and AlF_3 is unfavorable at all the temperatures shown in Figure 8. The ligand-exchange reaction between $SiCl_4$ and ZrF_4 or HfF_4 is feasible at >200 °C. The increasing negative ΔG for the ligand-exchange reaction between $SiCl_4$ and ZrF_4 or HfF_4 in Figure 8 is in agreement with the increasing etch rates at >250 °C displayed in Figure 9. The ZrO_2 etch rate is higher than the HfO_2 etch rate even though their predicted ΔG values are nearly equivalent. There must be additional kinetic factors that determine the actual etch rates.

Temperature and various metal precursors can also be used to tune the etch rate of a particular material. For example, the etch rates for Al_2O_3 ALE using various metal precursors are compared at different reaction temperatures in Figure 10. The ALE results for $Sn(acac)_2$ as the metal precursor were obtained

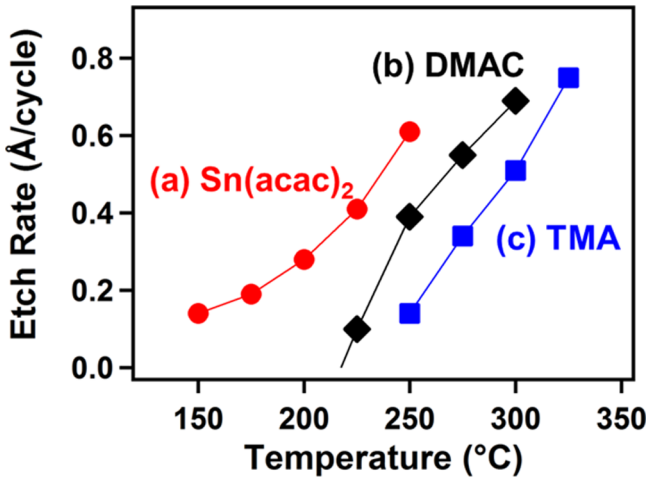

Figure 10. Etch rates of Al_2O_3 at different temperatures using (a) $Sn(acac)_2$, (b) DMAC and (c) TMA as the metal precursor.

earlier using a reaction sequence of 1−30−1−30.[8] The ALE results for TMA as the metal precursor were also measured earlier using a reaction sequence of 2−30−1−30.[11] The ALE results for DMAC as the metal precursor were obtained using a reaction sequence of 2−30−1−30. Each etch rate was measured using the mass change per cycle (MCPC) and the density of the Al_2O_3 film obtained by XRR.

The Al_2O_3 etching has different threshold temperatures for each metal precursor. The Al_2O_3 etch rates all increase at higher temperatures after exceeding the threshold temperature. Figure 10a shows that $Sn(acac)_2$ etched Al_2O_3 at temperatures ≥150 °C. In comparison, Figure 10b indicates that DMAC etched Al_2O_3 at higher temperatures ≥225 °C. Figure 10c shows that TMA etched Al_2O_3 at even higher temperatures ≥250 °C. The different temperature thresholds may be attributed to varying activation barriers for the ligand-exchange reactions. The different temperature thresholds for the etching may provide another method for obtaining selective thermal ALE.

IV. CONCLUSIONS

Selective thermal ALE can be accomplished by using different metal precursors for ligand exchange. This study explored selectivity in ALE using $Sn(acac)_2$, TMA, DMAC, and $SiCl_4$ as the metal precursors. These different metal precursors transfer acac, methyl, and chloride ligands during ligand exchange. Etching can occur if these ligands form stable and volatile reaction products during the ligand-exchange reaction. Differences between the stability and volatility of the possible reaction products can lead to selective etching.

This study examined the etching of Al_2O_3, HfO_2, ZrO_2, SiO_2, Si_3N_4, and TiN thin films on silicon wafers. All of the metal precursors etched HfO_2. All of the metal precursors also etched Al_2O_3 except $SiCl_4$. ZrO_2 was etched by all of the metal precursors except TMA. In contrast, none of the metal precursors could etch SiO_2, Si_3N_4, and TiN. The explanation for these results was based on the stability and volatility of the possible reaction products. The lack of etching of Al_2O_3 by $SiCl_4$ was explained based on thermochemical considerations.

Selective thermal ALE can also be achieved by tuning the reaction temperature. The etching of ZrO_2, HfO_2, and Al_2O_3

DOI: 10.1021/acs.chemmater.6b02543
Chem. Mater. 2016, 28, 7657−7665

using $SiCl_4$ as the metal precursor was consistent with thermochemical calculations. Temperature can be used to adjust the ZrO_2 etch rate relative to the HfO_2 etch rate using $SiCl_4$ as the metal precursor. The combination of different metal precursors and variable temperature can also tune the etch rate for Al_2O_3 ALE over a wide range of temperature.

The combination of different metal precursors with various ligands and different temperatures will provide pathways for selective thermal ALE. The selectivity in thermal ALE will complement the selectivity in ALD to provide for maskless processing. This selectivity will be important for atomic level processing to fabricate advanced semiconductor devices.

AUTHOR INFORMATION

Corresponding Author

*E-mail: steven.george@colorado.edu.

Notes

The authors declare no competing financial interest.

ACKNOWLEDGMENTS

This research was funded by Intel Corporation through a Member Specific Research Project administered by the Semiconductor Research Corporation. Additional support was provided by the National Science Foundation (CHE-1306131).

REFERENCES

(1) Carver, C. T.; Plombon, J. J.; Romero, P. E.; Suri, S.; Tronic, T. A.; Turkot, R. B. Atomic Layer Etching: An Industry Perspective. *ECS J. Solid State Sci. Technol.* **2015**, *4*, N5005−N5009.

(2) Kanarik, K. J.; Lill, T.; Hudson, E. A.; Sriraman, S.; Tan, S.; Marks, J.; Vahedi, V.; Gottscho, R. A. Overview of Atomic Layer Etching in the Semiconductor Industry. *J. Vac. Sci. Technol., A* **2015**, *33*, 020802.

(3) Agarwal, A.; Kushner, M. J. Plasma Atomic Layer Etching Using Conventional Plasma Equipment. *J. Vac. Sci. Technol., A* **2009**, *27*, 37−50.

(4) Oehrlein, G. S.; Metzler, D.; Li, C. Atomic Layer Etching at the Tipping Point: An Overview. *ECS J. Solid State Sci. Technol.* **2015**, *4*, N5041−N5053.

(5) George, S. M.; Lee, Y. Prospects for Thermal Atomic Layer Etching Using Sequential, Self-Limiting Fluorination and Ligand-Exchange Reactions. *ACS Nano* **2016**, *10*, 4889−4894.

(6) George, S. M. Atomic Layer Deposition: An Overview. *Chem. Rev.* **2010**, *110*, 111−131.

(7) Lee, Y.; DuMont, J. W.; George, S. M. Mechanism of Thermal Al_2O_3 Atomic Layer Etching Using Sequential Reactions with $Sn(acac)_2$ and HF. *Chem. Mater.* **2015**, *27*, 3648−3657.

(8) Lee, Y.; George, S. M. Atomic Layer Etching of Al_2O_3 Using Sequential, Self-Limiting Thermal Reactions with $Sn(acac)_2$ and HF. *ACS Nano* **2015**, *9*, 2061−2070.

(9) Lee, Y.; DuMont, J. W.; George, S. M. Atomic Layer Etching of HfO_2 Using Sequential, Self-Limiting Thermal Reactions with $Sn(acac)_2$ and HF. *ECS J. Solid State Sci. Technol.* **2015**, *4*, N5013−N5022.

(10) Lee, Y.; DuMont, J. W.; George, S. M. Atomic Layer Etching of AlF_3 Using Sequential, Self-Limiting Thermal Reactions with $Sn(acac)_2$ and Hydrogen Fluoride. *J. Phys. Chem. C* **2015**, *119*, 25385−25393.

(11) Lee, Y.; DuMont, J. W.; George, S. M. Trimethylaluminum as the Metal Precursor for the Atomic Layer Etching of Al_2O_3 Using Sequential, Self-Limiting Thermal Reactions. *Chem. Mater.* **2016**, *28*, 2994−3003.

(12) Osakada, K., Tranmetalation. In *Fundamentals of Molecular Catalysis, Current Methods in Inorganic Chemistry*; Kurosawa, H., Yamamoto, A., Eds.; Elsevier Science: Amsterdam, 2003; Vol. 3.

(13) Lockhart, J. C. Redistribution and Exchange Reactions in Groups IIB-VIIB. *Chem. Rev.* **1965**, *65*, 131−151.

(14) Elam, J. W.; Groner, M. D.; George, S. M. Viscous Flow Reactor with Quartz Crystal Microbalance for Thin Film Growth by Atomic Layer Deposition. *Rev. Sci. Instrum.* **2002**, *73*, 2981−2987.

(15) Lee, Y.; DuMont, J. W.; Cavanagh, A. S.; George, S. M. Atomic Layer Deposition of AlF_3 Using Trimethylaluminum and Hydrogen Fluoride. *J. Phys. Chem. C* **2015**, *119*, 14185−14194.

(16) Faraz, T.; Roozeboom, F.; Knoops, H. C. M.; Kessels, W. M. M. Atomic Layer Etching: What Can We Learn from Atomic Layer Deposition? *ECS J. Solid State Sci. Technol.* **2015**, *4*, N5023−N5032.

(17) *HSC Chemistry 5.1*; Outokumpu Research Oy: Pori, Finland.

(18) *CRC Handbook of Chemistry and Physics*, 96th ed.; Haynes, W. M., Ed.; CRC Press, LLC: Boca Raton, FL, 2015.

(19) Roesky, H. W.; Haiduc, I. Fluorine as a Structure-Directing Element in Organometallic Fluorides: Discrete Molecules, Supramolecular Self-Assembly and Host-Guest Complexation. *J. Chem. Soc., Dalton Trans.* **1999**, 2249−2264.

(20) Fahlman, B. D.; Barron, A. R. Substituent Effects on the Volatility of Metal Beta-Diketonates. *Adv. Mater. Opt. Electron.* **2000**, *10*, 223−232.

(21) Morozova, N. B.; Zherikova, K. V.; Baidina, I. A.; Sysoev, S. V.; Semyannikov, P. P.; Yakovkina, L. V.; Smirnova, T. P.; Gelfond, N. V.; Igumenov, I. K.; Carta, G.; Rossetto, G. Volatile Hafnium(IV) Compounds with Beta-Diketonate and Cyclopentadienyl Derivatives. *J. Phys. Chem. Solids* **2008**, *69*, 673−679.

(22) Bos, K. D.; Budding, H. A.; Bulten, E. J.; Noltes, J. G. Tin(II) Bis(1,3-Diketonates) and Tin(II) 1,3-Diketonate Chlorides. *Inorg. Nucl. Chem. Lett.* **1973**, *9*, 961−963.

(23) Kroll, W. R.; Kuntz, I.; Birnbaum, E. Investigation of Organoaluminum Beta-Diketonates. *J. Organomet. Chem.* **1971**, *26*, 313−320.

(24) Cox, M.; Lewis, J.; Nyholm, R. S. Complexes of Beta-Diketones with Group 4 Tetrachlorides. *J. Chem. Soc.* **1964**, 6113−6120.

(25) Pinnavaia, Tj; Fay, R. C. Preparation and Properties of Some 6- and 7-Coordinate Halo(acetylacetonato) Complexes of Zirconium-(IV) and Hafnium(IV). *Inorg. Chem.* **1968**, *7*, 502−508.

(26) Weidlein, J.; Krieg, V. Vibrational Spectra of Dimethyl and Diethyl Aluminum Fluoride. *J. Organomet. Chem.* **1968**, *11*, 9−16.

(27) Gundersen, G.; Haugen, T.; Haaland, A. Molecular-Structure of Dimethylaluminum Fluoride Tetramer, $[(CH_3)_2AlF]_4$. *J. Organomet. Chem.* **1973**, *54*, 77−86.

(28) Morrow, M. K. Synthesis and Characterization of Tetramethylhafnium. *Masters Thesis at University of Tennessee, Knoxville* **1970**, DOI: 10.2172/4153093.

(29) Wu, Y. D.; Peng, Z. H.; Chan, K. W. K.; Liu, X. Z.; Tuinman, A. A.; Xue, Z. L. Computational and Experimental Studies on the Thermolysis Mechanism of Zirconium and Hafnium Tetraalkyl Complexes. Difference Between Titanium and Zirconium Complexes. *Organometallics* **1999**, *18*, 2081−2090.

(30) Skinner, H. A. Thermochemistry of Organometallic Compounds. *J. Chem. Thermodyn.* **1978**, *10*, 309−320.

(31) Berthold, H. J.; Groh, G. Preparation of Tetramethylzirconium $Zr(CH_3)_4$. *Angew. Chem., Int. Ed. Engl.* **1966**, *5*, 516.

(32) Herzog, A.; Roesky, H. W.; Jager, F.; Steiner, A.; Noltemeyer, M. Reactions of $(h^5\text{-}C_5Me_5)ZrF_3$, $(h^5\text{-}C_5Me_4Et)ZrF_3$, $(h^5\text{-}C_5Me_5)_2ZrF_2$, $(h^5\text{-}C_5Me_5)HfF_3$, and $(h^5\text{-}C_5Me_5)TaF_4$ with $AlMe_3$. Structure of the First Hafnium-Aluminium-Carbon Cluster. *Organometallics* **1996**, *15*, 909−917.

(33) Murphy, E. F.; Lubben, T.; Herzog, A.; Roesky, H. W.; Demsar, A.; Noltemeyer, M.; Schmidt, H. G. First Mixed Fluoro-Chloro Group 4 Organometallics: Synthesis and Spectroscopic and Structural Characterization of $\{(C_5Me_5)ZrF_2Cl\}_4$, $\{(C_5Me_5)HfF_2Cl\}_4$, $(C_5Me_5)_4Zr_4(m\text{-}F)(m\text{-}F_2)_2(m\text{-}Cl)_2Cl_4$, $(C_5Me_5)_4Hf_4(m\text{-}F)_2(m\text{-}F_2)_2(m\text{-}Cl)_2Cl_4$, $(C_5Me_4Et)_2ZrClF$, and $(C_5Me_5)_2HfClF$. *Inorg. Chem.* **1996**, *35*, 23−29.

(34) Wailes, P. C.; Coutts, R. S. P.; Weigold, H. *Organometallic Chemistry of Titanium, Zirconium and Hafnium*; Academic Press, Inc.: New York, 1974.

DOI: 10.1021/acs.chemmater.6b02543
Chem. Mater. 2016, 28, 7657−7665

(35) Helms, C. R.; Deal, B. E. Mechanisms of the HF/H_2O Vapor-Phase Etching of SiO_2. *J. Vac. Sci. Technol., A* **1992**, *10*, 806−811.
(36) Kang, J. K.; Musgrave, C. B. The Mechanism of HF/H_2O Chemical Etching of SiO_2. *J. Chem. Phys.* **2002**, *116*, 275−280.
(37) Walsh, R. Bond-Dissociation Energy Values in Silicon-Containing Compounds and Some of Their Implications. *Acc. Chem. Res.* **1981**, *14*, 246−252.
(38) Ignatov, S. K.; Sennikov, P. G.; Chuprov, L. A.; Razuvaev, A. G. Thermodynamic and Kinetic Parameters of Elementary Steps in Gas-Phase Hydrolysis of SiF_4 Center Dot Quantum-Chemical and FTIR Spectroscopic Studies. *Russ. Chem. Bull.* **2003**, *52*, 837−845.
(39) Riley, R. F.; West, R.; Barbarin, R.; Slusarczuk, G.; Kirschner, S. Tris(Acetylacetonato)Silicon Chloride Hydrochloride and Some Derivatives. *Inorg. Synth.* **1963**, *7*, 30−34.
(40) Chakravarti, B. N. Preparation of Titanium (III) Acetylacetonate Tris(2,4-Pentanediono) Titanium (III). *Naturwissenschaften* **1958**, *45*, 286−286.
(41) Glaser, A.; Surnev, S.; Netzer, F. P.; Fateh, N.; Fontalvo, G. A.; Mitterer, C. Oxidation of Vanadium Nitride and Titanium Nitride Coatings. *Surf. Sci.* **2007**, *601*, 1153−1159.
(42) Piscanec, S.; Ciacchi, L. C.; Vesselli, E.; Comelli, G.; Sbaizero, O.; Meriani, S.; De Vita, A. Bioactivity of TiN-Coated Titanium Implants. *Acta Mater.* **2004**, *52*, 1237−1245.

DOI: 10.1021/acs.chemmater.6b02543
Chem. Mater. 2016, 28, 7657−7665